

Shock Detection and Design Enhancement for Pneumatic Control Valve

Wael Elmayyah

Assistant-Professor
Mechatronics Eng. Dpt.
Military Technical College
Cairo
Egypt

The existence of shockwaves in pneumatic valves can greatly affect their efficiency and cause damage to important parts. This study focuses on the examination of a cost-effective pneumatic directional control valve with the aim of augmenting its output mass flow rate. Emphasis is placed on scrutinizing and modifying the critical flow area to facilitate increased flow rates under specific upstream pressures while eliminating the formation of shockwaves.

To achieve these objectives, numerical simulations are harnessed to accurately capture the onset of shockwave formation and elucidate the associated conditions, allowing optimizing valve's capacity without introducing the risk of shockwave occurrence.

The modified valve design demonstrated the capability to eliminate shockwave formation within the valve while concurrently increasing the mass flow rate by up to 70% within the same range of inlet pressures. This novel approach holds substantial promise for enhancing system response and represents a significant contribution to the field of pneumatic control valve design.

Keywords: CFD, Pneumatic, Compressible flow, Shockwave, Control Valves.

1. INTRODUCTION

Digital position control circuits utilizing servo-pneumatic valves are commonly employed in various fields such as robotics, the automotive industry, and industrial automated productions, making them one of the most extensively utilized solutions. The key merits of servo-pneumatic systems lie in their cost effectiveness, precision, and performance, which contribute to their widespread application. In order to reduce the overall cost of a servo-pneumatic system without compromising control accuracy, the integration of low-cost on-off pneumatic control valves with digital control circuits has been widely adopted for this purpose [1, 2, 3]. Nevertheless, these cost-effective valves are constrained by their limited flow capacity. It is imperative to gain a comprehensive understanding of the internal air-flow behavior in order to optimize the valve characteristics, thereby enabling the system to achieve higher control accuracy. An increase in the output mass flow rate of a pneumatic valve at a constant inlet pressure has the potential to expedite the actuator and system response, thus enhancing overall performance.

In the process of examining valve design for an enhancement that takes into account the increase in valve capacity or the range of pressure, engineers may encounter challenges related to materials or flow. One of the difficulties related to flow in the design of valves is the avoidance of shock waves, which can have a detrimental effect on the valve components due to the presence of high turbulent flow. Computational fluid dynamics (CFD) is used to simulate internal compressible and incompressible flow [4] and analyze shock

waves and compressible flow in various scenarios [5]. Rossano and De Stefano simulate the early stages of aero-breakup of a water column due to a shock wave impact [6]. Khan et al. investigate the flow inside a supersonic nozzle and the formation of shock patterns using CFD techniques [7]. Mukhambetiyar et al. study unsteady compressible flow in micro shock tubes using CFD calculations [8]. Using numerical investigation and CFD, Bagheri et al. evaluate the effects of adding flow momentum on controlling oblique shock waves in a three-dimensional duct [9].

The formation of shockwaves within pneumatic valves can be analyzed through the use of computational fluid dynamics (CFD) [10]. CFD models that are based on the Reynolds Averaged Navier Stokes (RANS) equations and utilize the $k-\epsilon$ turbulence model have been employed to replicate the internal gas flow in safety relief valves [11]. These models have the capability to forecast the incidence and magnitude of shockwaves, in addition to other characteristics such as pressure peak and Mach number drop [12]. The design of control valves must take into consideration the geometrical and flow parameters that have an impact on the occurrence and intensity of shockwaves [13]. The consideration of these parameters is vital for ensuring the optimal performance and reliability of control valves in various industrial applications. The accurate prediction and mitigation of shockwave formations in valves are essential for preventing potential damage and ensuring the safe and efficient operation of the overall system. Therefore, a comprehensive understanding of the factors influencing shockwave occurrence and intensity is crucial for successfully designing and implementing effective control valves. The utilization of advanced computational tools and simulation techniques can greatly facilitate the analysis and optimization of valve designs with regard to shockwave prevention and management, thereby contributing to the enhanced performance and reliability of valve systems in diverse en-

Received: May 2023, Accepted: April 2024

Correspondence to: Dr Wael Elmayyah

Department of Mechatronics

Military Technical College, Cairo, Egypt

E-mail: Wael.Elmayyah@mtc.edu.eg

doi: 10.5937/fme2403382E

© Faculty of Mechanical Engineering, Belgrade. All rights reserved

FME Transactions (2024) 52, 382-392 382

gineering applications. In addition, computational fluid dynamics (CFD) has been employed to enhance valve functionality through the alteration of the internal flow pathway, leading to a higher mass flow rate, as indicated by Chun et al. [14]. Furthermore, empirical investigations have been carried out to examine the impact of the duration of valve opening on the formation of shockwaves. By simulating the fluid behavior and analyzing the valve's performance, the critical air mass flow rate of a control valve can be determined with great precision [15-19]. Computational Fluid Dynamics (CFD) models have the capability to accurately predict the pressure drop, flow force, and mass flow rate at various valve positions, thereby providing valuable insights into the behavior of the valve. Moreover, these models offer the opportunity to optimize the performance of the valve by implementing design modifications that enhance its flow characteristics. For instance, adjustments such as rounding sharp edges, eliminating dead spaces, and minimizing abrupt changes in direction can be made to improve the overall efficiency of the valve. It is important to note that experimental tests are frequently employed to validate the findings derived from CFD simulations, thus ensuring the dependability and accuracy of the predictions. This multi-faceted approach combines simulation and experimental validation and is essential for advancing the understanding and performance optimization of control valves in practical applications. On the whole, CFD serves as a valuable instrument for comprehending and enhancing the performance of pneumatic valves in the presence of shockwaves, thus contributing to the advancement of the field. Consequently, CFD is a crucial tool in the analysis and optimization of pneumatic valve behavior, particularly in the context of shockwave interactions, and its significance cannot be overstated in the realm of engineering.

For sonic and supersonic internal flow, the mass flow rate is determined by the critical area where the flow is choked, i.e., the Mach number equals one [20]. Once the flow is choked, the mass flow rate is dependent on upstream pressure and the critical flow area regardless of the downstream flow conditions. For a typical spool-type pneumatic directional control valve, the critical area is the narrowest area between the spool and the valve's land. The impact of rounding the sharp bed corner on the output mass flow rate has been investigated by [21] and Whitehead et al. [13]. They concluded that rounding the sharp edges of the valve's internal geometry leads to a mass flow increase. However, by investigating the internal airflow through the valve [22, 23], the risk of the formation of a shockwave appeared at the rounded corner

Computational Fluid Dynamics (CFD) can offer a visual and quantitative assessment of internal flow inside pneumatic valves by modeling the internal gas flow. This assessment can be used to identify and eliminate shock waves [24, 25]. Reynolds Averaged Navier Stocks (RANS) equations along with the $k-\epsilon$ turbulence model were used for these purposes in [7, 23, 26-28]. Moreover, the works of Whitehead et al. [13] and Naveen et al. [29] are good examples of optimizing

the geometrical design of servo-valves for better performance using CFD. However, the scope of these studies was constrained to enhancing the valve's performance without incorporating a novel design that could enhance the response of the valve while also considering the possibility of mitigating shock wave effects. The main aim of the current investigation is to enhance the flow rate of output in a pneumatic control valve without causing internal shock waves. This particular objective is pursued through the strategy of dividing the area of the single annular outlet port into smaller apertures. To accomplish this, a commercial computational fluid dynamics (CFD) tool is utilized to visualize the internal flow characteristics, capture the shock waves that may form, and evaluate the effectiveness of the design alterations. The remaining sections of this manuscript are structured in the following manner. Firstly, the pneumatic valve under investigation in the case study is introduced, followed by a comprehensive discussion of the research methodology employed. Subsequently, the findings of the investigation are detailed and analyzed. Finally, the paper concludes with the presentation of the primary conclusions drawn from the study and the corresponding recommendations for future research and practical applications.

2. CASE STUDY VALVE AND METHODOLOGY

The valve under investigation is a low-cost, on-off pneumatic directional control valve. It is a 3/2 solenoid operated with an internal pneumatic pilot with spring return. In a study conducted by Yousry et al. [30], a pair of these valves were utilized to control a double-acting pneumatic cylinder in order to enhance the accuracy of position control. In order to accurately predict the mass flow rate of the valve's outlet mass flow rate, the researchers employed an experimental setup, as depicted in Figure 1, in conjunction with a validated dynamic mathematical model of the system [31] that was solved using Simulink R2019b in MATLAB R2019b. Figure 1 shows the controlled double-acting cylinder (1), which is fitted with an LVDT (Linear Variable Differential Transformer) that has a nominal displacement of 100 mm, 4.8 KHz operating frequency, nominal output voltage span (0.5:10) Volt, and operated by 15:30 dc volt; two-directional control valves (2) to control the extension and retraction of the cylinder, the working pressure range of the valve is from 0.7 bar minimum to 10 bar maximum pressure, this valve is the one under study; three pressure transducer (3) to measure the air pressure at the pressurized air source (s) and the cylinders' ports. The first two pressure transducers are identical programmable Parker transducers analog/digital output, with the ability to adjust the output voltage to an adjusted pressure range, i.e., a pressure range can be selected to be from 0 to 10 bar with output from 0 to 5 Volt, with response time ≤ 2.5 ms. The third pressure transducer, PES-110, only has an analog output and operating pressure of 0 to 10 bar. The feedback signals of the three pressure transducers and the cylinder's LVDT are connected to a commercial open-source microcontroller, ATmega-328, on Arduino Uno (4), which manages the control signals to the valve's solenoids according to the control algo-

rithm. In addition, the feedback data from the three pressure transducers and the LVDT are connected to a data acquisition card (DAQ) (5); the DAQ has 64 analog inputs at up to 100 KS/s, 16-bit resolution with input range from ± 0.1 to ± 10 Volt, and absolute accuracy 2.119 mV for voltage range from 0 to 5 Volt, and 8 digital I/O lines (TTL/CMOS); two 24-bit counter/timers. That is connected to a PC (6) to store the data to be used with the Simulink model. The Figure shows the valve's ISO symbol, while Figure 2 (a) provides a diagrammatic representation of the internal flow area of the valve. As the valve has three ports and two positions, the flow through the valve has only two directions: Pressurised air flows either from the pressurized air source port (P) to the actuator port (A) or from the actuator port (A) to exhaust port (T). To direct the air from P to A, a pilot air signal pushes the valve spool up against the spring. This pilot signal is allowed only if the on-off solenoid is activated. Therefore, when the solenoid is deactivated, the pilot signal flow is cut off, and the spring returns the spool to the normal position to allow the airflow from the actuator port (A) to the exhaust port (T). In both cases, the airflow goes through an expansion process, i.e., from high pressure that approaches the inlet pressure value to low pressure that approaches atmospheric pressure. These flow conditions may lead to the formation of shock waves. Youssry et al. [30, 32] have previously presented a comprehensive analysis of the valve's construction and test rig details, offering detailed insights into its design and functionality.

The critical area of the valve inner passage is $5.93e-06 \text{ m}^2$. As stated earlier, the objective of the present study is to increase the outlet mass flow rate at a given inlet pressure while eliminating the formation of shock waves. Therefore, four designs, along with the original design, have been investigated. In each case, the impact of changing the critical flow area's location and size has been examined. Case 01 is modified from the original design by rounding (radius = 0.5 mm) the sharp edges of the spool land at Area 1 and Area 2, as shown in Figure 2(b). Figure 3 shows the mesh of the 3D half model of the different studied Cases. Case 01 outlet port shown in Figure 3 is a single large outlet area. In Cases 02 to 04, the single outlet port of Case 01 has been

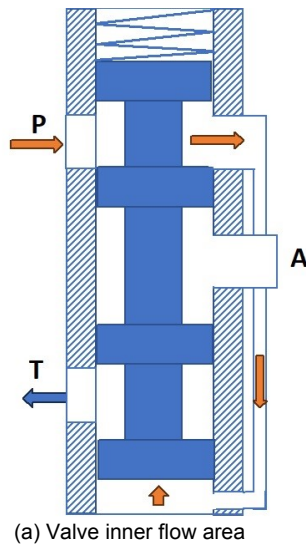


Figure 2. Flow area of the valve

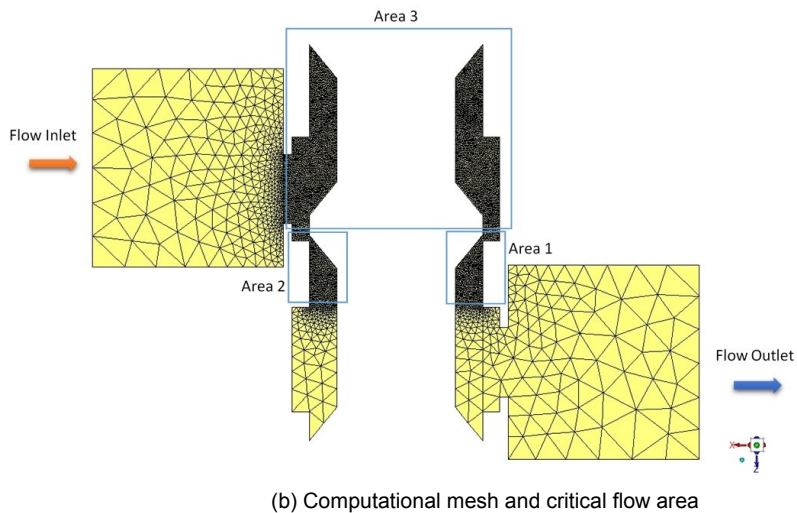
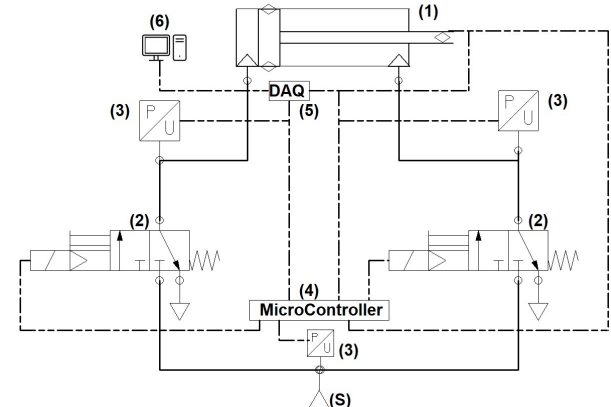


Figure 1. Experimental test rig arrangement

modified to a set of eight smaller ports (holes) of different diameters, as shown in Figure 3. For all cases, the range of inlet flow pressure investigated is 2 to 10 bar.

The critical case takes place during the two operating positions, either from the high-pressure air source to a low-pressure actuator's chamber or from a pressurized actuator to the atmosphere. Due to the symmetry of the valve under study, the geometry and the flow area are the same in both cases. Therefore, the inlet and outlet ports of the valve around the spool are modeled. As the valve has a symmetric design, only half the 3D model of the valve is considered. Four different computational domains are built, one for each design. The computational domains are discretized into over 260K tetrahedral cells with higher density in flow areas of interest identified as area1 (exit-wise), area2 (inlet-wise), and Area3, Figure 2(b). The insensitivity of simulation results to spatial resolution is confirmed via a grid sensitivity check. A more dense mesh of 354781 tetrahedral cells has been used to examine the grid independence, with no significant improvement for the solution. The difference in air mass flow rate between the inlet and outlet was 0.000001 kg/s , so the cell number was kept at about 260K in all cases. Boundary conditions were applied at the inlet, outlet, and walls of the valve, with the walls being defined as stationary. At the inlet, the stagnation pressure, static pressure, and stagnation temperature were applied, along with initial values for turbulence intensity and hydraulic diameter.



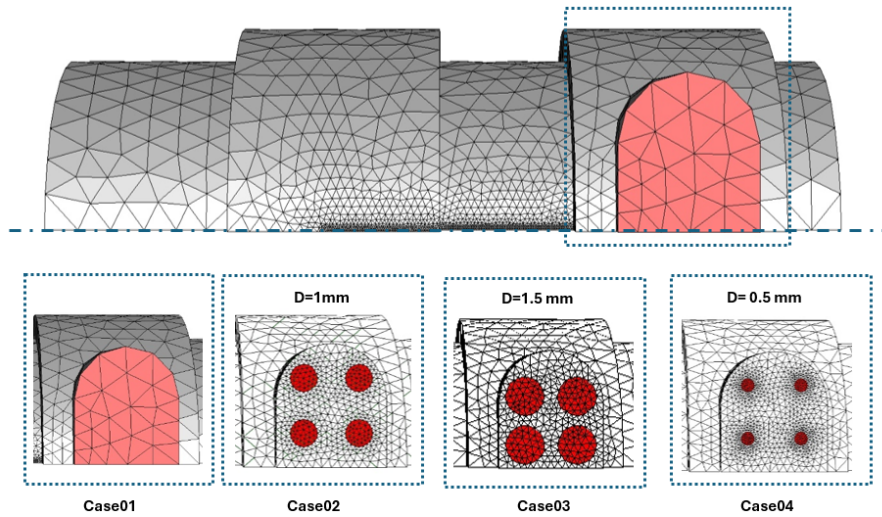


Figure 3. Computational mesh of the studied cases

This allowed an initial mass flow rate to be estimated at the inlet, which was then recalculated based on downstream conditions at the choking plane. At the outlet, the static pressure and stagnation temperature were applied as boundary conditions. However, the flow calculation was independent of the outlet boundary condition because the flow was choked for all test pressures in the study. A discretization scheme with second-order upwind convection terms and second-order central difference diffusion terms for the continuity, momentum, energy, turbulent kinetic energy, and turbulent dissipation energy equations has been used. The convergence criterion was based on the residual values of the calculated variables, with threshold values of $1e-3$, except for the energy equation, which had a threshold of $1e-6$.

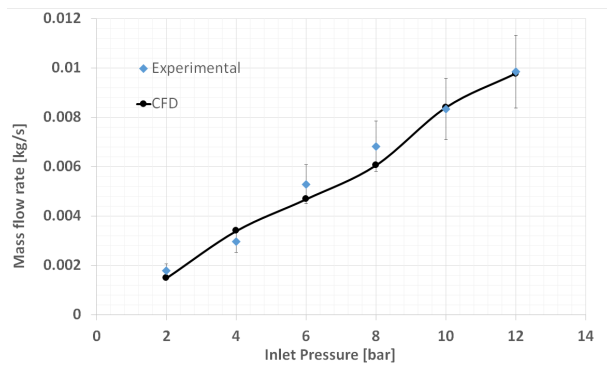


Figure 4. Comparison of the experimental results and the CFD predicted values

The pressure range studied was from 2 to 10 barg. Overall, a total of 20 simulation experiments are planned. In all simulations, air, the working fluid, is treated as a compressible ideal gas.

A commercial CFD simulation tool, ANSYS 19.2, Fluent 19.2, is utilized [33, 34]. To validate simulation results, experimental tests are conducted on the original valve. These tests were reported in [35, 30], finding good agreement for mass flow rate at different pressure ranges. Figure 4 shows the comparison between the experimental and the computational model predicted values of mass flow rate at different inlet pressure values. It can be noticed from Figure 4 that the predicted results are within

15% of the experimental results as they fall within the 15% error bars. The maximum difference value ranges from 0.75 kg/s at an inlet pressure of 12 bar and 16.6 kg/s at an inlet pressure of 2 bar; this ratio to the experimental results makes an error percent of 2% to 15%, which shows a prediction accuracy of the computational model ranges from 85% to 98%.

A linear regression for the experimental and computational results have been carried out. Equ (1a) and equ (1b) represent the linear equation that represent the experimental results and the computational results with the associated The coefficient of determination (R^2).

$$\dot{m} = 0.0008P - 0.0001 \quad R^2 = 0.9934 \quad (1a)$$

$$\dot{m} = 0.0008P - 0.00001 \quad R^2 = 0.9941 \quad (1b)$$

where \dot{m} is the air mass flow rate (kg/s) and P is valve the inlet pressure (bar). The difference between the two lines is a fixed value of $1.5e-4$ which could represent an error of 2% which indicates accuracy of 98%.

3. RESULTS AND DISCUSSION

3.1 Shockwave Analysis of Case 01

The distribution of flow pressure and Mach number through a pneumatic valve can be used to predict the critical flow area that controls the mass flow rate and to detect the presence and location of shock waves, as well as their intensity. As a sample, the Case 01 design operating at 10 bar inlet pressure is examined. Figures 5a and 5b illustrate the Mach contours at areas 1 and 2, respectively, in design Case 01 at a valve inlet pressure of 10 bar. The corresponding static pressure contours on the valve side at area 1 and area 2 are illustrated in Figures 6a and 6b, respectively.

By closely examining the two figures, it can be shown that the flow is choked at plane C, denoted by the solid line C-C where $M=1$. In area 1, Figure 5a, the Mach number increases from zero to reach the value of 3.22 then suddenly drops with a large decreasing gradient to 0.6, which indicates the occurrence of a local normal shockwave at the location of the dashed line B-B. In area 2, Figure 5b, the Mach number increases from

zero to reach the value of 2.15, then suddenly drops with a large decreasing gradient to 0.8, which indicates the occurrence of a shockwave at the location of the dashed line A-A. Along the valve side, the pressure value is reduced from 10 to 0.2 bar. After the dashed line location, a positive gradient is noticed going from 0.1 to 6.0 bar, indicating a shock wave's occurrence. It can be concluded that there are two critical locations in the airflow

path; the first one is where the flow is choked, which is crucial for controlling the mass flow rate; the other location is where the shockwave takes place, which involves a high risk of flow disturbance and valve damage. This can be better illustrated by tracking the static pressure and Mach number values downstream along the valve spool's surface at the Shockwave location at Area 1, shown in Figure 7.

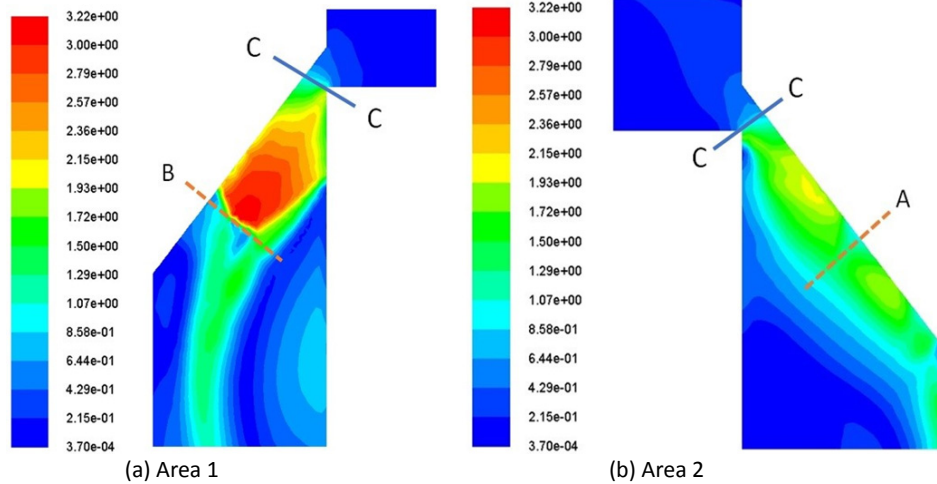


Figure 5. Mach number distribution at 10 bar, Case 01

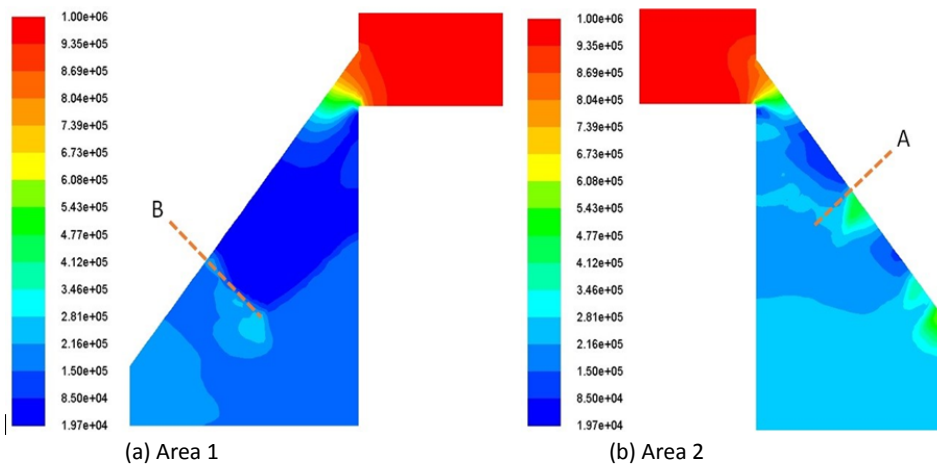


Figure 6. Static pressure distribution at 10 bar, Case 01

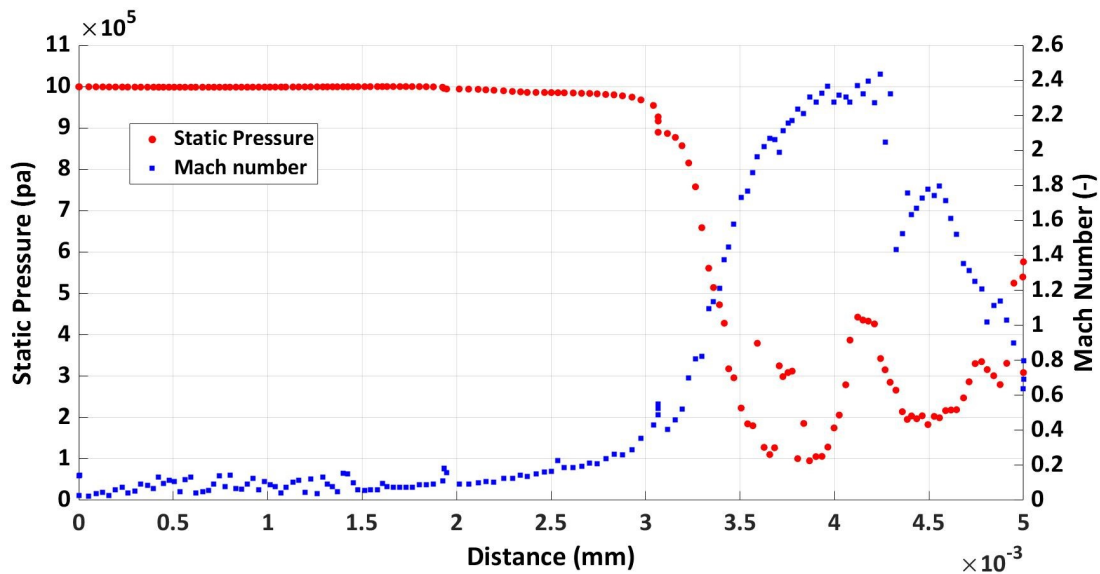


Figure 7. Mach number and Static Pressure at the location of the Shockwave (Case 01 at 10 bar).

One important remark can be addressed by examining the Mach number and static pressure distribution in Areas 1 and 2 in Figures 5 and 6 and comparing the locations of the choked area and the shockwave location. The choking and shock wave areas are not 2D plan areas; rather, they are 3D annulus asymmetric areas around the spool.

Figure 8 illustrates the impact of inlet pressure on pressure and Mach number upstream-to-downstream ratios and their gradients along the spool; the latter indicates the severity of the shockwave. By comparing values, it is confirmed that the formation of Shockwaves with higher intensity occurs at higher inlet pressures.

Nonetheless, due to increasing inlet pressure, the undesirable formation of shockwave is associated by the desirable increase in mass flow rate. For instance, by increasing inlet pressure from 4 bar to 6 bar, a shock wave pressure gradient is increased by 66% whereas the mass flow rate is increased by 50%.

3.2 Impact of Valve Geometry Modifications

As concluded above, increasing the mass flow rate (via increasing inlet pressure) in Case 01 is associated with the formation of shockwaves. It is desired that the mass flow rate be increased while eliminating the shock wave formation. Therefore, three modifications to the valve outlet area are carried out. The modifications are to divide the outlet port area into eight smaller holes while reducing the outlet area, as stated in Table 1. The outlet area size of Case 02 has been designed to be close to the value of the critical Area of Case 01, while the outlet areas in the other cases have been designed to be larger (case 01) and smaller (case 04) than the critical Area of Case 01. Pressure distribution, Mach number, and mass flow rate were investigated in the three cases from 02 to 04, with inlet pressure ranges from 2 to 10 bar. By doing this modification, the critical flow area has been moved from the plane C-C (Figures 5a and 5b) to the new smallest area, i.e., the outlet area; Figure 9 shows the mass flow rate at different valve inlet pressure for the four modified cases along with the original design. Case 04 was ignored in the further investigation as it led to a dramatic decrease in mass flow rate. It could be noticed that the slope of each case is directly proportional to the critical flow area size. The highest slope is Case 03, which has the largest flow critical area, while Case 04 has the lowest area and, hence, the lowest slope. This confirms that at a given inlet pressure, the mass flow rate depends on the inlet pressure value and the critical flow area. The slope values of Case 01 and Case 02 are close to each other as the critical flow area difference between them is very small; however, they are different in shape and location. Figure 9 shows that.

Case 03 has the largest flow rate; It ranges from 0.01 to 0.03 kg/s, which is an increase of 0.007 to 0.015 kg at the same pressure as the original design Case 01. This increase percent is ranging from 98.2 to 235.2 % if it is compared to the original design Case 01 flow rate at the same inlet pressure and it ranges from 49.5 to 70 % if it is compared to Case 03 flow rate.

By moving the critical area to the exit rather than the spool land, flow choking no longer takes place at the

spool land. Rather, flow chokes at exit holes. This is evident by examining the Mach contours and the static pressure distribution along the symmetry plane and the Mach contours at the valve outlet ports.

Figures 10 and 11 show the Mach number distribution along the symmetry plane of Case 02 and Case 03, respectively. It could be noticed that there is no sign of the choking plan or the shockwave. More importantly, airflow is maintained subsonically all through the valve, and internal shocks have been totally eliminated. However, because of the larger outlet flow area at Case 03, the Mach number value approaches one at flow Area 1, shown in Figure 11(b), which indicates that the flow choking could take place at this location if a larger outlet area is allowed.

Table 1. Investigated Geometrical Cases

Case	Hole Diameter (mm)	Outlet Area (m ²)	Critical area (m ²)
01	Annulus Area	1.62832E-5	5.9286E-06
02	1	6.28571E-06	6.28571E-06
03	1.5	1.41429E-05	1.41429E-05
04	0.5	1.57143E-06	1.57143E-06

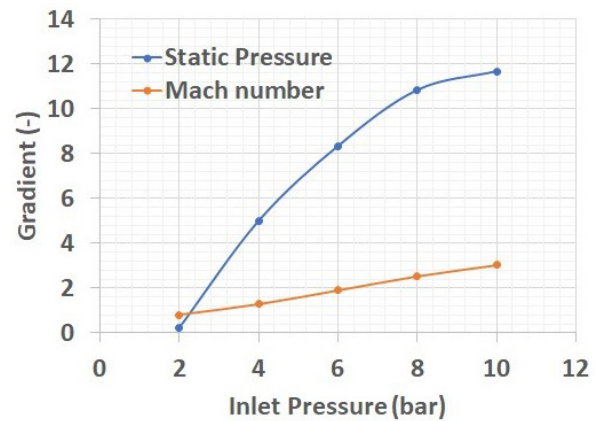


Figure 8. Mach number and static pressure gradient at the Shockwave location (Case 01 at 10 bar).

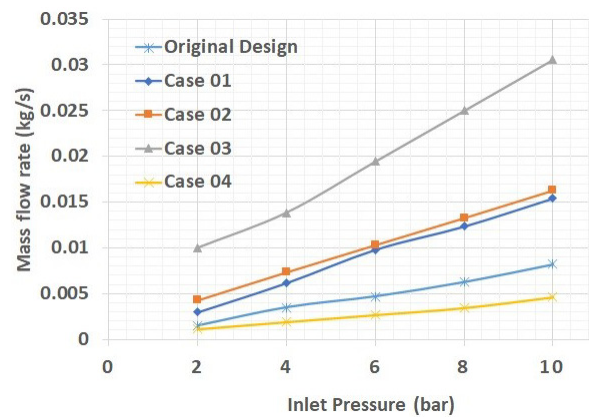


Figure 9. Air mass flowrate at different inlet pressure

For further investigations to confirm the elimination of the shockwave, the static pressure distribution along the symmetry plane of Case 02 and Case 03 are shown in Figures 12 and 13, respectively. For Case 02, Figure 12 shows nearly a single static pressure value, whereas for the larger outlet area in Case 03, Figure 13 shows a smooth pressure drop along the symmetry plane. The Mach number distribution of the outlet ports in Case 02

and Case 03, shown in Figure 14, indicates the formation of the choking area at the outlet ports at the Mach number value of 1.

Figures 15 and 16 show the Mach number values and the static pressure downstream along the surface of the valve spool land at the same location of the shockwave occurred at Case 01 for inlet pressure of 10 bar. It is clear that for Case 02 and Case 03 at the maximum inlet pressure, no sudden increase in the pressure nor sudden drop in Mach number took place.

All of these results confirm the migration of choking area to outlet holes and the disappearance of the shockwave inside the valve. This is also associated with the advantage of mass flow rate increase for the same inlet pressure. In Case 03, the flow rate has been increased with no formation of shockwaves. Therefore, the flow can be increased and optimized for the same inlet pressure by optimizing the flow geometry and adjusting the critical flow area.

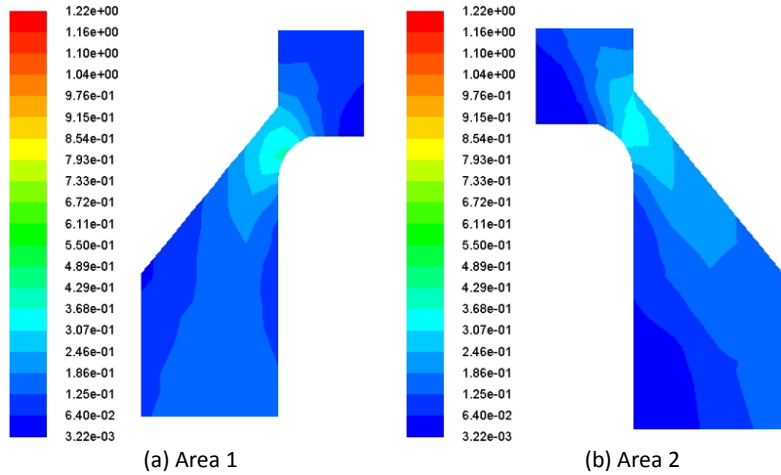


Figure 10. Mach number distribution at 10 bar, Case 02

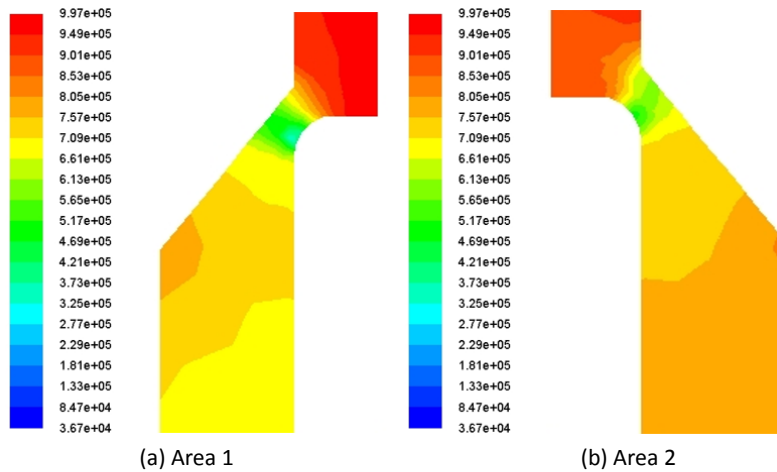


Figure 11. Mach number distribution at 10 bar, Case 03

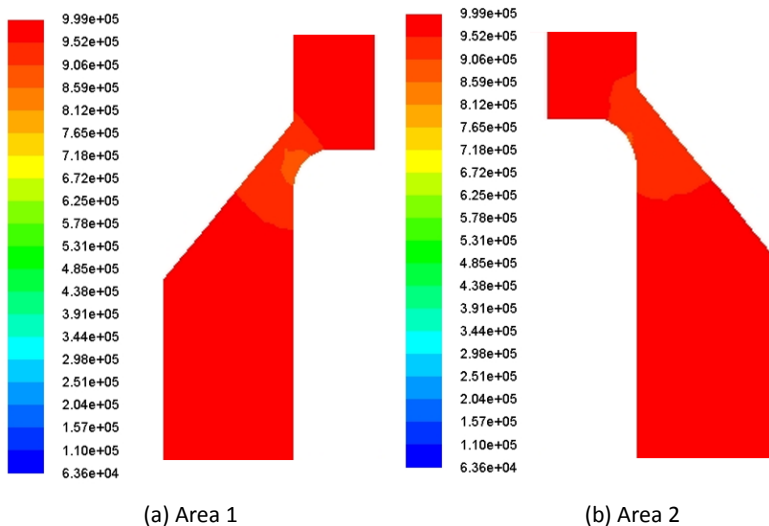


Figure 12. Static Pressure distribution at 10 bar, Case 02

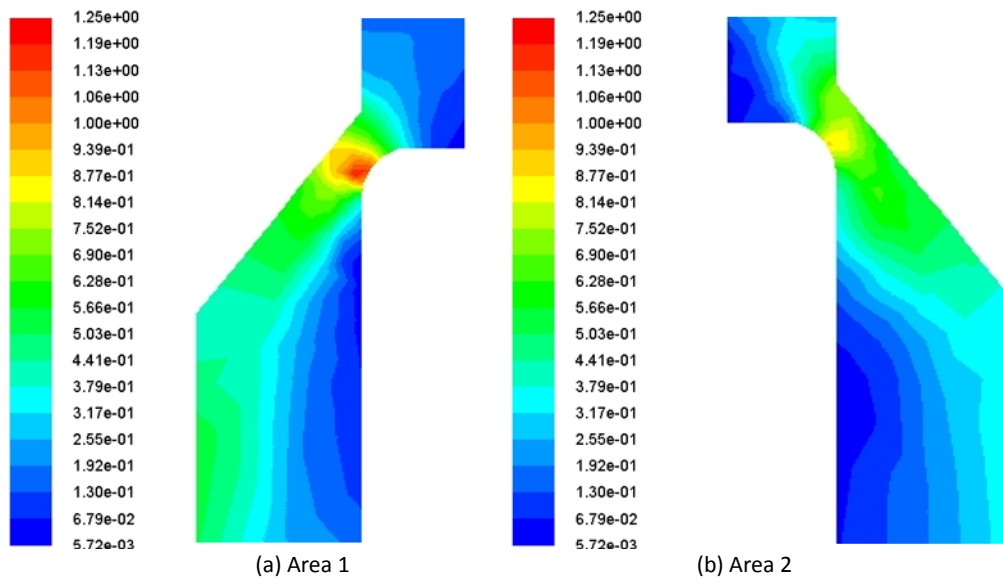


Figure 13. Static Pressure distribution at 10 bar, Case 03

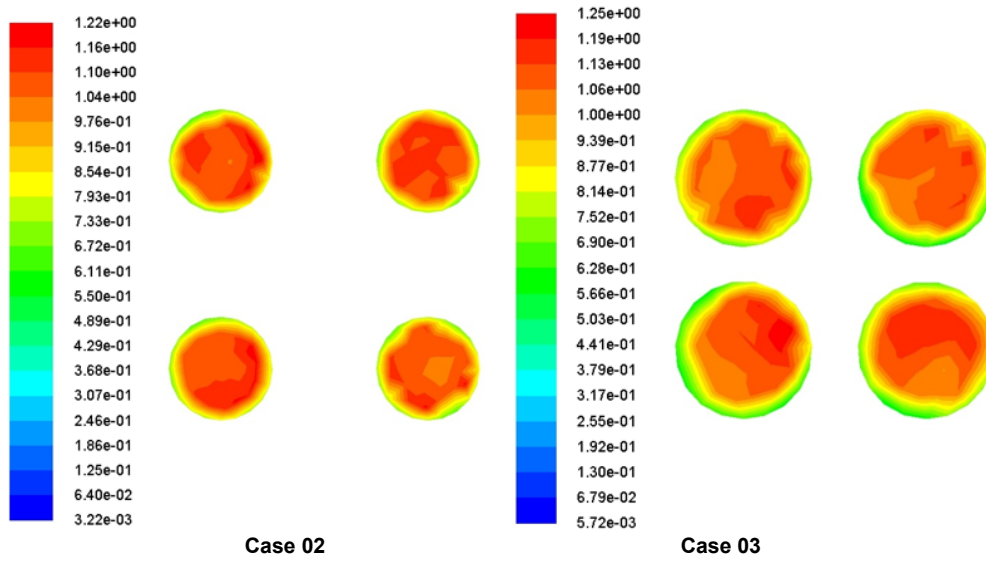


Figure 14. Mach number distribution at 10 bar at the flow outlet

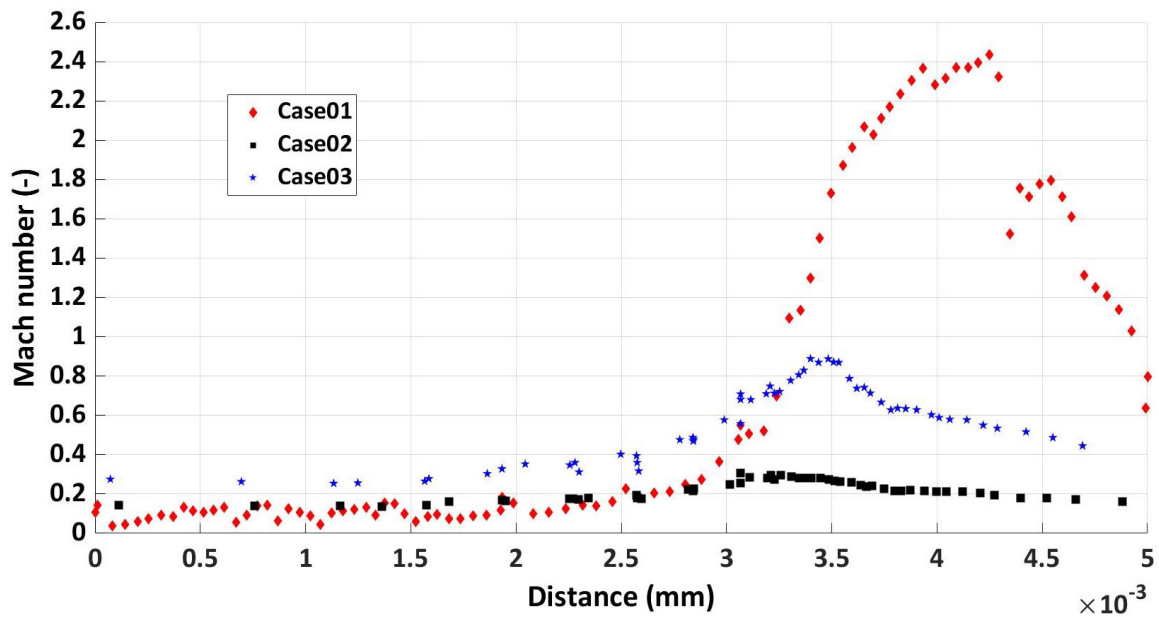


Figure 15. Mach number at the location of the shockwave (10 bar).

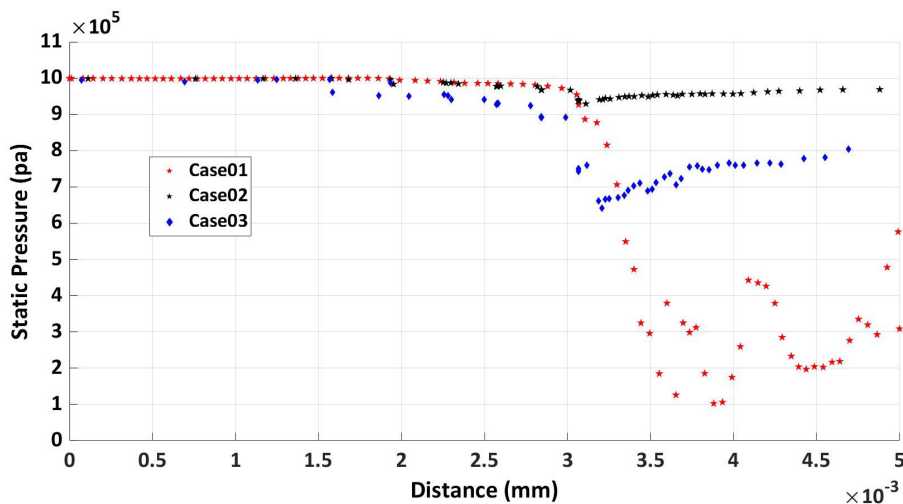


Figure 16. Static pressure at the location of the shockwave (10 bar).

4. CONCLUSIONS

A low-cost pneumatic directional control valve has been investigated to improve its performance by increasing the output air mass flow rate at the same inlet pressure. A modified design for the valve has been proposed and investigated using CFD. The computational model has been validated by comparing its predicted results with experimental results. Three different cases of the modified design, in addition to the original design, have been investigated. In the modified design, the outlet port area has been modified from a fully open area to eight smaller holes. Each case has a different hole diameter and, hence, a different outlet flow area. All cases have been investigated for the range of inlet pressure from 2 to 10 barg. The critical flow areas have been identified: the choked area where the Mach number equals one and the location of a local shock wave. It has been shown that modifying the outlet area could control the mass flow rate and prevent the formation of shockwaves. With this modification, the choking area has been relocated to the modified valve outlet holes, and there is no shockwave formation inside the valve. Also, the modified valve design increases the mass flow rate by up to 70% at the same inlet pressure range, which could enhance the system response. Investigating the internal flow can detect the location and intensity of shockwaves and identify the critical flow area. By relocating the choked area in sonic and supersonic flow, the formation of shockwaves could be eliminated while increasing the mass flow rate.

REFERENCES

[1] Shen, X., 2010, "Nonlinear model-based control of pneumatic artificial muscle servo systems," *Control Engineering Practice*, 18 (3), mar, pp. 311–317.

[2] Azahar, M. I. P., Irawan, A., Taufika, R. M., and Suid, M. H., 2020, "Position control of pneumatic actuator using cascade fuzzy self-adaptive PID," In *Lecture Notes in Electrical Engineering*. Springer Singapore, pp. 3–14.

[3] Zou, Q., 2021, "Extended state observer-based finite time control of electro-hydraulic system via sliding mode technique," *Asian Journal of Control*, aug.

[4] Habeeb, L. J., Saleh, F. A., Maajel, B. M., 2019, "Cfd modeling of laminar flow and heat transfer utilizing Al_2O_3 /water nanofluid in a finned-tube with twisted tape," *FME Transactions*, 47 (1), pp. 89–100.

[5] Kostic, O., Stefanovic, Z., Kostic, I., 2015, "Cfd modeling of supersonic airflow generated by 2d nozzle with and without an obstacle at the exit section," *FME Transactions*, 43 (2), pp. 107–113.

[6] Rossano, V., Stefano, G. D., 2021, "CFD prediction of shock wave impacting a cylindrical water column," In *Computational Science and Its Applications – ICCSA 2021*. Springer International Publishing, pp. 376–386.

[7] Khan, S. A., Ibrahim, O. M., Aabid, A., 2021, "CFD analysis of compressible flows in a convergent-divergent nozzle," *Materials Today: Proceedings*, 46, pp. 2835–2842.

[8] Mukhambetiyar, A., Jaeger, M., Adair, D., 2017, "CFD modeling of flow characteristics in micro shock tubes," *Journal of Applied Fluid Mechanics*, 10 (4), Jul, pp. 1061–1070.

[9] Bagheri, H., Mirjalily, S. A. A., Oloomi, S. A. A., Salimpour, M. R., 2021, "Effects of flow momentum enhancement using an artificial external source on shock wave strength, a CFD study," *Acta Astronautica*, 187, oct, pp. 70–78.

[10] Elmayyah, W., 2013, "Computational fluid dynamics investigations of shock waves in safety relief valves," *International Conference on Aerospace Sciences and Aviation Technology*, 15 (AEROSPACE SCIENCES), may, pp. 1–11.

[11] Chochia, G. A., Tilley, D. G., and Schaefer, H. N., 2001, "Numerical and experimental investigations on a shock wave related cavitation flow," *Proceedings of the Institution of Mechanical Engineers, Part I: Journal of Systems and Control Engineering*, 215 (1), Feb, pp. 71–91.

[12] Lee, D. W., Park, J. M., Kwon, Y. D., Kwon, S. B., 2008, "Effect of rupture disc curvature on the compression waves in s/r valve," *Journal of Mechanical Science and Technology*, 22 (4), apr, pp. 755–760.

- [13] Whitehead, N. P., Slaouti, A., Taylor, H., 2007, "Optimisation of flow through a pneumatic control valve using CFD analysis and experimental validation," *International Journal of Fluid Power*, 8 (3), Jan, pp. 31–41.
- [14] Chunsik, S., Junchang, J., Heedong, K., 2009, "Numerical simulation of the film rupture process of shock wave tube flow," *Journal of the Korean Society of Propulsion Engineering*, 13 (1), pp. 27–33.
- [15] Rumyantsev, V. V., Lushcheko, V. A., Mavleev, I. R., Pavlenko, A. P., 2023, "Variable nozzle turbocharger: gas-dynamic calculation, 3d modeling, CFD analysis, characteristics," *Trudy NAMI(1)*, apr, pp. 6–18.
- [16] Arab, M. A., Gamil, A. I., Syam, T., Umer, M., Ghani, S., 2021, "Air expulsion analysis of an industrial air valve using CFD," In 2021 12th International Conference on Mechanical and Aerospace Engineering (ICMAE), IEEE.
- [17] Garcia-Todoli, S., Iglesias-Rey, P., Mora-Melia, D., Martinez-Solano, F., and Fuertes-Miquel, V., 2018, "Computational determination of air valves capacity using CFD techniques," *Water*, 10 (10), oct, p. 1433.
- [18] Fresia, P., Rundo, M., 2021, "CFD simulation of a post-compensated load sensing directional control valve," *E3S Web of Conferences*, 312, p. 05002.
- [19] Li, S., Wu, P., Cao, L., Wu, D., She, Y., 2017, "CFD simulation of dynamic characteristics of a solenoid valve for exhaust gas turbocharger system," *Applied Thermal Engineering*, 110, jan, pp. 213–222.
- [20] Beater, P., 2007, *Pneumatic Drives* Springer Berlin Heidelberg.
- [21] Dempster, W., Lee, C. K., Deans, J., 2006, "Prediction of the Flow and Force Characteristics of Safety Relief Valves," *Proceedings of PVP2006-ICPVT-11 2006 ASME Pressure Vessels and Piping Division Conference*, July.
- [22] He, M., Lu, W., Xu, Z., Xing, P., 2018, "Characteristics analysis of shock wave near nozzle in ejector," *IOP Conference Series: Earth and Environmental Science*, 189, nov, p. 022065.
- [23] Raghu, A., Kumar, Y. V. N., 2018, "Numerical investigation on effect of divergent angle in convergent-divergent rocket engine nozzle," *Chemical Engineering Transactions*, 66, pp. 787–792.
- [24] Wu, Z., Xu, Y., Wang, W., Hu, R., 2013, "Review of shock wave detection method in CFD postprocessing," *Chinese Journal of Aeronautics*, 26 (3), June, pp. 501–513.
- [25] Knight, D., Yan, H., Panaras, A. G., Zheltovodov, A., 2003, "Advances in CFD prediction of shock wave turbulent boundary layer interactions," *Progress in Aerospace Sciences*, 39 (2-3), Feb., pp. 121–184.
- [26] Qian, J.-y., Wei, L., Jin, Z.-j., Wang, J.-k., Zhang, H., Lu, A.-l., 2014, "CFD analysis on the dynamic flow characteristics of the pilot-control globe valve," *Energy Conversion and Management*, 87, Nov., pp. 220–226.
- [27] Vu, B., Wang, T.-S., Shih, M.-H., Soni, B., 1994, "Navier-Stokes flow field analysis of compressible flow in a high pressure safety relief valve," *Applied Mathematics and Computation*, 65 (1-3), pp. 345–353.
- [28] Davis, J. A., Stewart, M., 2002, "Predicting globe control valve performance-part i: CFD modeling," *Journal of Fluids Engineering*, 124 (3), aug, pp. 772–777.
- [29] Naveen, K. K., Vijayanandh, R., Ramesh, M., 2019-11, "Design optimization of nozzle and second throat diffuser system for high altitude test using CFD," *Journal of Physics: Conference Series*, 1355, p. 012012.
- [30] Youssry, M. A., Mahgoub, H. M., Mabrouk, M. H., Elmayyah, W. M., 2016, "Design and simulation of mechatronic systems, pneumatic positioning application," Master's thesis, Mechanical Engineering.
- [31] Elmayyah, W., Samy, M., 2023, "Reduced order model for an electro-hydraulic valve of a gas turbine engine's controller," *FME Transactions*, 51(2), pp. 169–175.
- [32] Youssry, M., Elmayyah, W., Mabrouk, M., Mahgoub, H., 2016, "Parametric study of a low cost pneumatic system controlled by on/off solenoid valves," *International Journal of Research in Engineering and Technology*.
- [33] Hinze, J., 1975, *Turbulence*, 2 ed. McGraw-Hill Inc., US.
- [34] Ansys *ANSYS Fluent Theory Guide*.
- [35] Youssry, M., Elmayyah, W., Mabrouk, M., 2020, "Position control of a pneumatic cylinder actuator using modified PWM algorithm," *Journal of Engineering Science and Military Technologies*, 4 (1), pp. 121–126.

NOMENCLATURE

M	Mach Number (-)
\dot{m}	Air Mass flow rate (kg/s)
$M1/M2$	Mach number ratio upstream to downstream the shockwave (-)
P	Pressure (pa)
$P1/P2$	Pressure ratio upstream to downstream the shockwave (-)
R^2	The coefficient of determination (-)

ДЕТЕКЦИЈА УДАРА И ПОБОЉШАЊЕ ДИЗАЈНА ЗА ПНЕУМАТСКИ КОНТРОЛНИ ВЕНТИЛ

В. Елмајах

Постојање ударних таласа у пнеуматским вентилима може у великој мери утицати на њихову ефикасност и изазвати оштећења важних делова. Ова студија се фокусира на испитивање исплативог пнеуматског усмереног вентила са циљем повећања његовог

излазног масеног протока. Нагласак је стављен на испитивање и модификовање критичног подручја протока како би се олакшале повећане брзине протока под специфичним узводним притисцима док се елиминише формирање ударних таласа.

Да би се постигли ови циљеви, нумеричке симулације су упрегнуте како би се тачно ухватио почетак формирања ударног таласа и разјаснили повезани услови, омогућавајући оптимизацију

капацитета вентила без увођења ризика од појаве ударног таласа.

Модификовани дизајн вентила показао је способност елиминисања формирања ударних таласа унутар вентила док истовремено повећава масени проток до 70% у оквиру истог опсега улазних притисака. Овај нови приступ обећава значајно побољшање одзива система и представља значајан допринос области дизајна пнеуматских контролних вентила.